Carbohydrate Polymers 87 (2012) 2263–2269

Contents lists available at SciVerse ScienceDirect

Carbohydrate Polymers

journal homepage: www.elsevier.com/locate/carbpol

Radiation synthesis, characterization and dye adsorption of alginate–organophilic montmorillonite nanocomposite

Manal F. Abou Taleb[a,b,*], Dalia E. Hegazy[a], Sahar A. Ismail[a]

[a] National Center for Radiation Research and Technology, P. O. Box No. 29, Nasr City, Cairo, Egypt
[b] Faculty of Science and Humanities Studies, Salman Bin Abdul Aziz University, Alkharj, Saudi Arabia

ARTICLE INFO

Article history:
Received 11 October 2011
Received in revised form 18 October 2011
Accepted 22 October 2011
Available online 28 October 2011

Keywords:
Nanocomposites
OMMT
γ-Ray irradiation
TEM
Adsorption
Anionic dyes

ABSTRACT

In this paper, the preparation, characterization and dye adsorption properties of nanocomposite (calcium alginate/organophilic montmorillonite) (CA/OMMT) were investigated. A new nanocomposite consisting of alginate and OMMT was prepared by polymerization using γ-rays irradiation as initiator. Physical characteristics of CA/OMMT were studied using X-ray diffraction (XRD), infrared spectrophotometery (IR), thermal gravimetric analysis (TGA), transmission electron microscopy (TEM) and the corresponding selected area electron diffraction (SAED). Two textile dyes, acid green B and direct pink 3B, were used as model anionic dye. Factors affecting dye sorption, such as pH, sorbent concentration and temperature of each dye solution were extensively investigated. It was found from the study that the sorption of dyes by the nanocomposite is pH-dependent and maximum sorption was obtained at pH 2. The thermodynamic data showed that dye adsorption onto alginate was spontaneous, exothermic, and a physisorption reaction. On the basis of the data of the present investigation, one could conclude that the as-prepared adsorbents exhibited excellent affinity for the dye, and can be applied to treat wastewater containing anionic dyes.

1. Introduction

Dyes have been the subject of many interests in recent years because of increasingly stringent restrictions on the organic content of industrial effluents (Abou Taleb, Abd El-Mohdy, & Abd El-Rehim, 2009). Dyes are one of the most hazardous chemical compound classes found in industrial effluents and need to be treated since their presence in water bodies reduces light penetration, precluding the photosynthesis of aqueous flora (Royer et al., 2009). They are also aesthetically objectionable for drinking and other purposes (Royer, Cardoso, Lima, Macedo, & Airoldi, 2010). Dyes can cause allergy, dermatitis, skin irritation (Brookstein, 2009) and also provoke cancer and mutation in humans (Carneiro, Umbuzeiro, Oliveira, & Zanoni, 2010).

The most efficient method for the removal of synthetic dyes from aqueous effluents is the adsorption procedure (Olivares-Marín et al., 2009; Calvete, Lima, Cardoso, Dias, & Pavan, 2009). This process transfers the dyes from the water effluent to a solid phase, thereby keeping the effluent volume to a minimum (Cuerda-Correa, Domínguez-Vargas, Olivares-Marín, & de Heredia, 2010; Malarvizhi & Ho, 2010). Subsequently, the adsorbent can be regenerated or stored in a dry place without direct contact with the environment (Calvete et al., 2010a; Calvete, Lima, Cardoso, Dias, & Ribeiro, 2010b). From the view of industrial application, removal of dyes by adsorption is a promising approach because of its low performance cost and easy technical access (Kumar, Ramamurthi, & Sivanesan, 2005). In addition, the adsorption processes give the best results as they can be used to remove different types and concentrations of dyes, providing an attractive treatment, especially if low-cost adsorbents are used. Many adsorbents have been employed to remove dyes from effluents.

Very recently, the application of hydrogels as adsorbents has been paid special attention. Hydrogels with three dimensional crosslinked polymeric structures and hydrophilic groups can swell considerably in aqueous solution without dissolution because hydrophilic chains contact one to the other by cross-links (Sannino et al., 2005). Hydrogels have many predominant properties including low interfacial tension and a variety of functional groups which can trap ionic dyes from wastewater and endowed hydrogels with high adsorption capacities, which is a favor for the treatment of the environment (Yi & Zhang, 2008). But pure hydrogels often have some limitations such as low mechanical stability and gel strength and introduction of clays materials into hydrogels can overcome these drawbacks because hydrogels with clays materials combine elasticity and permeability of the gels with high ability of the clays to adsorb different substances (O¨ztop, Hepokur, & Saraydin, 2010). As a consequence, much research concerning hydrogels with clays

* Corresponding author at: P.O. Box 29, Nasr City, Cairo 11731, Egypt. Tel.: +20 1 21423531; fax: +20 2 22749298.
E-mail address: abutalib_m@yahoo.com (M.F. Abou Taleb).

0144-8617/$ – see front matter © 2011 Elsevier Ltd. All rights reserved.
doi:10.1016/j.carbpol.2011.10.058

Dyes	Structure formula
Acid Green B	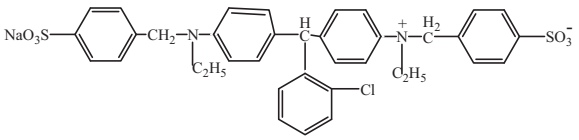
Direct Pink 3B	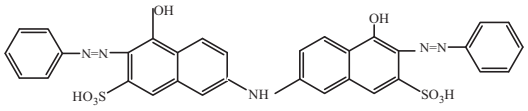

Chart 1. Chemical structure of dyes.

materials adsorbing dyes (Kaşgöz & Durmus, 2008) and metal ions (Chen & Wang, 2009) have exponentially increased.

The organoclay is a very important application of clay minerals and has been widely used as adsorbents of organic pollutants in soil, water and air. An interesting phenomenon has been observed that organic modification can significantly improve the clay's adsorption capability toward anionic dyes. However, investigations on the adsorption mechanism of this process are relatively scarce. At present, the main mechanism proposed is believed to be the binding between anionic groups (e.g., sulfonic groups) of the dye and the positively charged surface of organoclays (Zhu & Ma, 2008; Pulikesi, Ramamurthi, & Sivanesan, 2006). Recent research about the adsorption of anionic dyes on organoclays rarely deals with the effect of the loading of organic cations on the dye's removal.

Alginate is a naturally occurring carbohydrate polymer and has a capacity to remove toxic pollutants. One of the important properties of alginate is the ability to form hydrogels (Jankowski, Zielinska, & Wysakowska, 1997). An aqueous solution of alginate is readily transformed into a hydrogel on addition of metallic divalent cations such as Ca^{2+}. Calcium alginate immobilized microbial cultures have been used for decoloration of dyes (Aravindhan, Fathima, Rao, & Nair, 2007; Ramsay, Mok, Luu, & Savage, 2005). The aim of this study is to focus a synthesized CA/OMMT nanocomposites initiated by γ-ray irradiation polymerization. The objectives of this study are to investigate the effects of the prepared nanocomposite on the structural, thermal, and the retention of anionic dye pollutants such as acid green B and direct pink 3B dyes using CA/OMMT nanocomposites.

2. Materials and methods

2.1. Chemicals

Sodium alginate (SA) and triethyl amine used in this study were a laboratory grade chemicals obtained from Aldrich Chemical Co. (Milwaukee, WI, USA) and used as received. The clay mineral used in this study was sodium montmorillonite. Two different types of dyes were used as adsorbents. The dyes used in the experiments were acid green B (λ_{max} = 636 nm) and direct pink 3B (λ_{max} = 526 nm). Dyestuffs and Chemicals Co., Kaffer El-Dawar, Egypt supplied all of these dyes. The chemical structures of different dyes are depicted in Chart 1. All of the dyes were commercial grade and were used without any further purification. The other chemicals and phosphate buffers were reagent grade and used as received. In addition, distilled water was used as a solvent. Structures of the dyes are shown.

2.2. Preparation of reactive intercalating agents for clay

Vinyl benzyl triethyl ammonium chloride (VBTAC) was prepared according to Mulvancy and Chang (1977).

2.3. Modification of clay (OMMT)

The cation exchange procedure was followed using previously described methods (Al-Sigeny, Abou Taleb, & El-Kelesh, 2009).

2.4. Synthesis of CA/OMMT nanocomposites

An exact amount of alginate (SA) was first dissolved in distilled water to prepare 3 wt% solutions. The nano particle loadings were varied as 0%, 1%, 3% and 5% OMMT of the combined weight of the SA. After constant stirring for 30 min, the system was deoxygenated by degassed for 10 min. Irradiation to the required doses (20 kGy) was carried out in a ^{60}Co gamma cell (made in Russia) facility of the National Center for Radiation Research and Technology, Cairo, Egypt at a dose rate of 2.86 Gy/s. $CaCl_2$ (3 wt%) was used in the final feeding solutions of hydrogels, after gamma irradiation, to form network structure of calcium alginate (CA). After completion of the reaction, the contents were cooled and cast on a glass plate, the solvent was then evaporated and sample films were obtained.

2.5. Instrumentation

The XRD analysis was performed using XD-DI Series, Shimadzu apparatus using nickel-filtered and Cu-Kα target.

FTIR spectra were recorded on Mattson 1000, Unicam infrared spectrophotometer Cambridge, England in the range from 400 to 4000 cm^{-1} using KBr pellets.

Thermogravimetric analyzer Shimadzu TGA system of Type TGA-50 was used in this study. The temperature range was from ambient to 600 °C at heating rate of 10 °C/min in nitrogen atmosphere 20 mL/min.

The surface morphology of the copolymer was examined with a Jeol JSM-5400 scanning electron microscopy (SEM) (JEOL, Tokyo, Japan).

TEM measurements: The as-prepared powders were suspended in ethanol and a drop of the resultant mixture was deposited on an ultra thin carbon supported Cu grid, and air-dried. Energy-filtered electron powder diffraction used TEM JEOL: JEM-100cx.

Absorbance measurement was carried out on UNICAM UV–Vis Spectrometer. 1000 Model spectrophotometer.

2.6. Water uptake measurements

The clean, dried sample nanocomposites of known weights were immersed in distilled water at 25 °C until equilibrium was reached (almost 24 h). The samples were removed, blotted quickly with absorbent paper and then weighed. The uptake percentage of these samples was calculated using the equation:

$$\text{Water uptake\%} = \frac{w_s - w_d}{w_d} \times 100$$

where w_d and w_s represent the weights of dry and wet sample nanocomposites, respectively.

2.7. Adsorption studies

Adsorption isotherms were determined by the batch method for all adsorbents. Accurately weighted dry samples (0.1 g) were placed in a solution of a definite volume (25 mL) and allowed to stand for a period of 4 days at room temperature. Adsorption amount of dye (mg/g) was calculated by using the following equation:

$$q_e = \frac{[(C_0 - C_e) \times V]}{W}$$

where W is the weight of dry (CA/OMMT) nanocomposites (g); V is the volume of the aqueous phase (L); q_e is the amount of dye

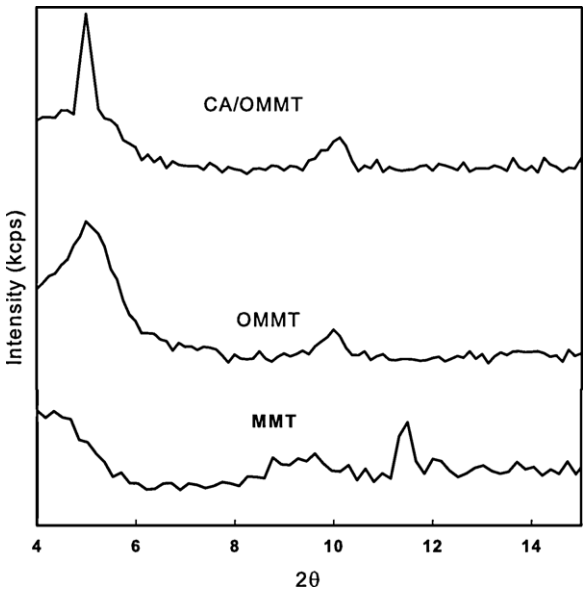

Fig. 1. XRD patterns of MMT and OMMT and CA/OMMT nanocomposites, at 5 wt% of OMMT.

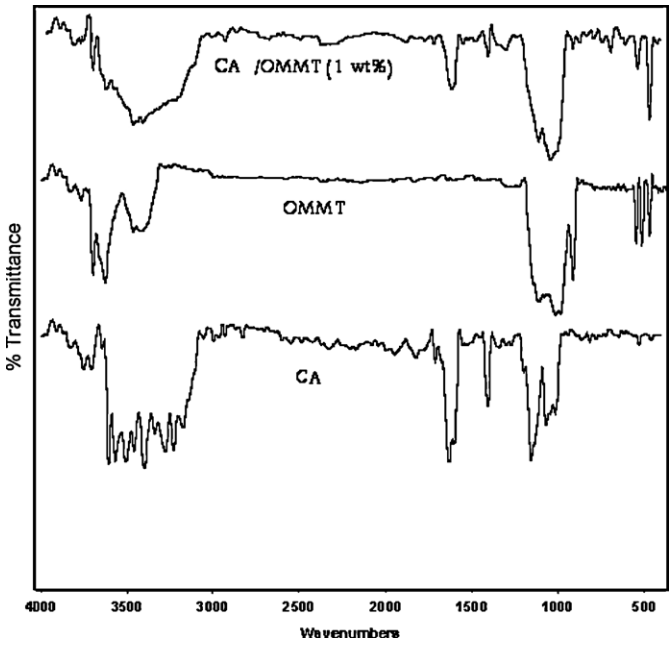

Fig. 2. FTIR spectra of CA, OMMT and CA/OMMT.

adsorbed onto unit dry mass of the (CA/OMMT) nanocomposites (mg/g^1), C_0 and C_e are the concentrations (mg/L) of the dye solution before and after adsorption, respectively, that were determined by using an UNICAM UV–VIS spectrophotometer (1000 Model spectrophotometer) at identical dye's absorbance wavelengths. It was then computed to dyes concentrations using a standard calibration curve.

2.8. Desorption and regeneration studies

The reusability of the adsorbent mainly depends on the ease with which dyes are desorbed from loaded CA/OMMT nanocomposites sample. For this 20 mL of 100 ppm dyes solution was treated with 0.1 g of CA/OMMT nanocomposites and was kept for 24 h. The content of the flask was filtered and separated. The filtered adsorbent was retreated with 100 mL neutral distilled water and distilled water adjusted to different pH with the addition of 1 M HCl and 1 M NaOH. It was stirred for 24 h. The residual dyes concentration was measured. The study was carried out at room temperature ($25 \pm 2\,^{\circ}C$).

The total uncertainty for all experiments was in the range 3–4%.

3. Results and discussions

The nanocomposites were synthesized using γ-ray irradiation as free radical initiator and crosslinking agent. The OMMT can be used as a crosslinking agent due to quaternary ammonium in OMMT containing double bonds (C=C), which can react with the alginate monomer to form gel. (Weian, Wei, & Yue'e, 2005) In addition, the OMMT opens the gallery spacing, which allowed monomers, and polymers to enter more easily. Calcium chloride (3 wt%) was incorporated after irradiation to crosslink the alginate chains. The presence of nitrogen atom "N" was confirmed by elemental analysis.

The evidence for the intercalated structure of nanocomposites can be obtained by XRD. Fig. 1 shows the X-ray diffraction patterns of Na–MMT, OMMT and (CA/OMMT) nanocomposites as a certain weight sample 5 wt%. The diffraction peak of the OMMT occurring at $2\theta = 5.3624^{\circ}$, corresponding to 15.7 Å, shifted from that of Na-MMT ($2\theta = 11.389^{\circ}$), corresponding to 7.7633 Å. These indicated that the cation exchange is intercalated into the galleries of silicate layers after exchanging with the sodium ion. Thus, montmorillonite is successfully modified by the surfactant and OMMT is formed. After polymerization with alginate, the characteristic peak related to clay is not disappeared and still present in position $2\theta = 5.36^{\circ}$. Accordingly, it is suggested that the OMMT silicate sheets are intercalated in CA/OMMT nanocomposites. This in turn, results in an increase in basal spacing of OMMT and CA/OMMT from 15.7 Å to 17 Å as interplaner distance between the faces of their lamellar crystals.The FTIR spectra of CA, OMMT, and CA/OMMT nanocomposites are shown in Fig. 2 which clearly confirm the presence of CA, OMMT and CA/OMMT. FTIR spectrum of calcium alginate (Fig. 2) shows absorption bands at 3450 cm^{-1} (OH stretching), 1618 cm^{-1} (COO– asymmetric stretching), and 1412 cm^{-1} (COO– symmetric stretching). The bands at 1125 cm^{-1} are due to the –C–O stretching of ether groups and the bands at 1065 cm^{-1} are assigned to the –C–O stretching of alcoholic groups (Vijaya, Popuri, Boddu, & Krishnaiah, 2008). In cases of nanocomposite and OMMT, the characteristic transmittance bands of –MMT (OH stretching at 3634 cm^{-1}, Si–O stretching at 1043 cm^{-1}, Al–O stretching at 518 cm^{-1}, and Si–O bending at 462 cm^{-1}) were observed. These bands confirm the presence of –MMT in the OMMT and CA/OMMT nanocomposites. Further, the appearance of a peak in the range of 800–850 cm^{-1} is attributed to p-disubstituted benzene. This peak confirms the presence of an aromatic ring of VBTAC. Similar peaks in the spectra of poly-VBTAC have been reported by Hummel (1991). Also, the peak in the range of 1580–1641 cm^{-1} is attributed to the $-COO^{-}$ group and thus it confirms the presence of the carbonyl group of alginate (Kolhe & Kumar, 2007).

3.1. TEM

More information about the microstructures of CA/OMMT nanocomposites containing 5.0 wt% organophilic clay was obtained by TEM observations. The suspended phase of CA/OMMT nanocomposites was shown in Fig. 3(a). Many dark, as distinct spherical particles were distributed in the micrograph. Surprisingly, the silicate layers in the OMMT nanocomposites are randomly distributed and their particles are not equally uniformed throughout the OMMT particle matrix.

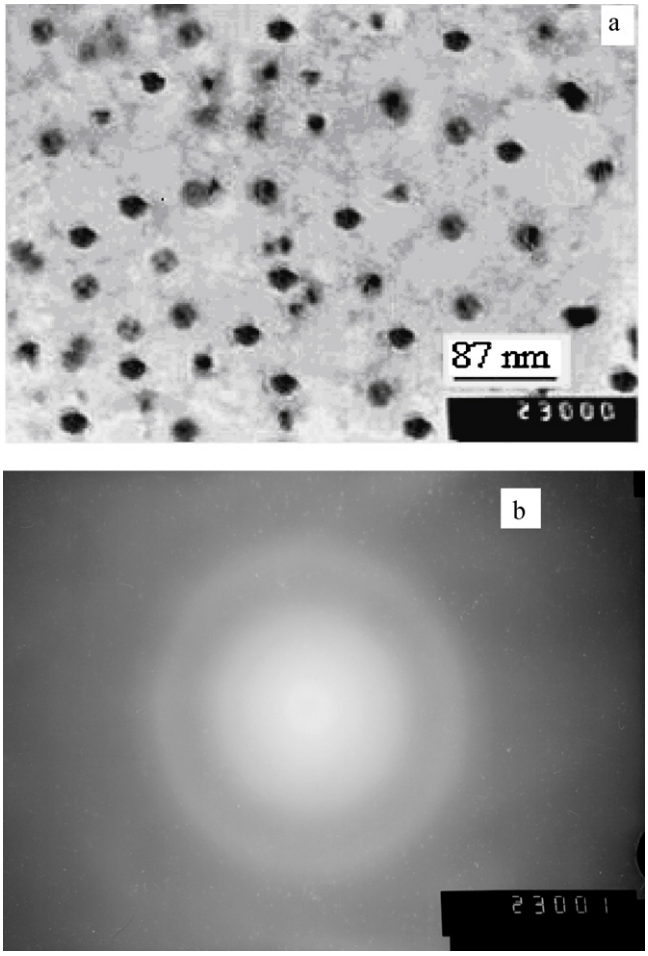

Fig. 3. (a) TEM micrograph and (b) the selected area electron diffraction pattern of CA/OMMT nanocomposites with 5.0 wt % of OMMT.

Fig. 3(b) shows the corresponding selected area electron diffraction (SAED) pattern. Distribution of the particles at random and small particles causes the widening of diffraction rings that made up of many diffraction spots, which indicate that the nanoparticles are polycrystalline structure (Zhou et al., 2009). Electron diffraction reveals that each particle is composed of many small crystal nuclei, which is a convincing proof that the particles grow in an aggregation model.

3.2. Thermal analysis

Thermogravimetric analysis (TGA) of the prepared polymeric ammonium (CA/OMMT) nanocomposites at different weights of OMMT were measured under a nitrogen atmosphere in the temperature range 30–600 °C in order to investigate the thermal stability. TGA data in Fig. 4 indicates that the 5 wt% OMMT nanocomposite

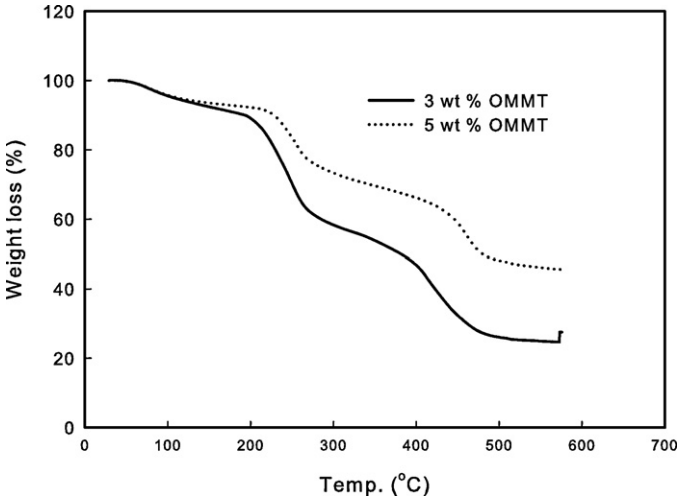

Fig. 4. Thermogravimetric analysis of CA/OMMT nanocomposites, at different weights of OMMT.

decompose at a higher temperature in three stages with good thermal properties if compared with the 3 wt% OMMT which undergo decomposition at relatively low temperature. It indicates that the increase of OMMT concentration in nanocomposite exhibited an enhanced thermal stability. This improvement in thermal stability may attribute to the inherently good thermal properties of inorganic clays and the probable intercalation of polymer into interlamellar clay layers (Min, Wang, Hui, & Jie, 2006) prevents the heat to be transmitted quickly, and limited any further continuous decomposition of the nanocomposites. The clay layers may hinder the diffusion of volatile decomposition products (Li, Yu, & Yang, 2005).

As shown in Fig. 4, the residual weight percentages at 400–600 °C for OMMT (3 wt%), and (5 wt%) were 23, and 49 wt%, respectively. The residual weight % for the nanocomposite mainly resulted from the undecomposed –MMT, and it increased with the increasing –MMT content.

3.3. Water uptake studies

Table 1 shows the percentage of water uptake for the CA/OMMT nanocomposites. It can be seen that the water uptake percentage of the nanocomposites decreases with OMMT increasing. It is perhaps because that the crosslinking density increases and the pores of the nanaocomposites become smaller, which is not fit for water absorbency.

3.4. Adsorption studies

3.4.1. Effect of OMMT content (wt%) on adsorption

Fig. 5 shows the effect of wt% on adsorption capacities of CA/OMMT nanocomposites for the anionic dyes such as acid green

Table 1
Water absorption, thermodynamic parameters and effect of temperature on the amount adsorption of dyes on CA/OMMT nanocomposites with different contents of OMMT.

OMMT conc. (wt %)	Water uptake (%) 24 h	Amount adsorption of dyes (mg/g)											
		Acid green B						Direct red 3B					
		Temperature (°C)			Thermodynamic parameter			Temperature (°C)			Thermodynamic parameter		
		30	40	50	ΔH kJ mol^{-1}	ΔG kJ mol^{-1}	ΔS eu.	30	40	50	ΔH kJ mol^{-1}	ΔG kJ mol^{-1}	ΔS eu.
1	1010.2	12	16.5	13	–	–	–	10	14	11.6	–	–	–
3	998.8	28	35	30	−42.6	−2.4	46	20	28.3	22.8	−33.2	−3.355	37
5	985.42	26	31	28.8	–	–	–	16	24.0	18.0	–	–	–

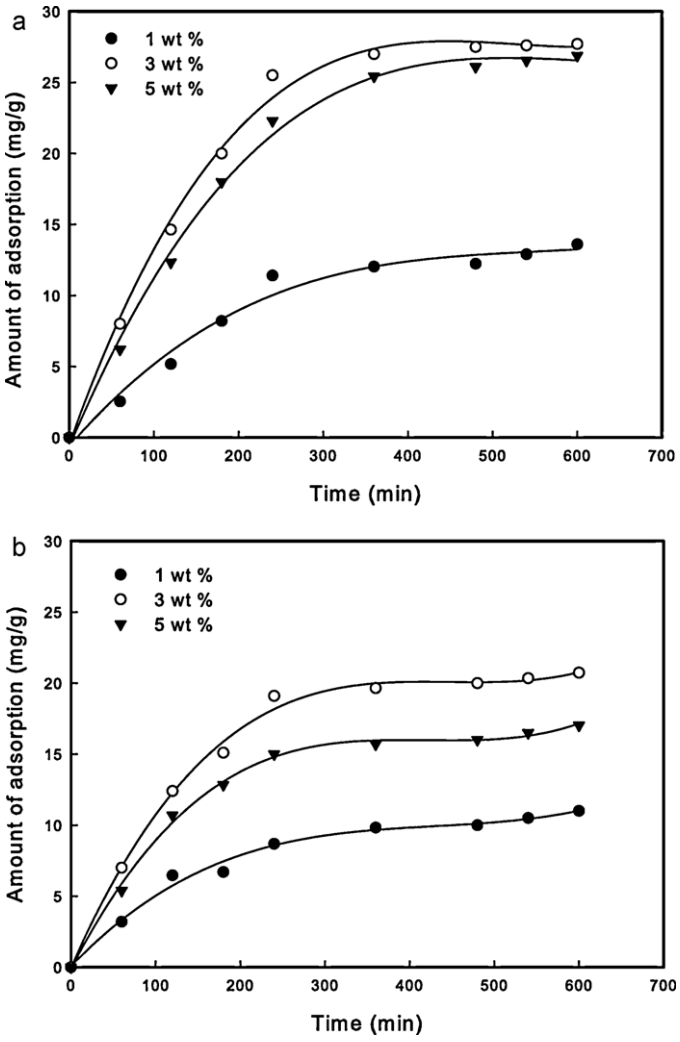

Fig. 5. Effect of the time (min) on adsorption capacity of CA/OMMT nanocomposites with different content of OMMT, for different dyes. Conc.: 100 mg/L; temp.: 30 °C (a) acid green B (b) direct pink 3B.

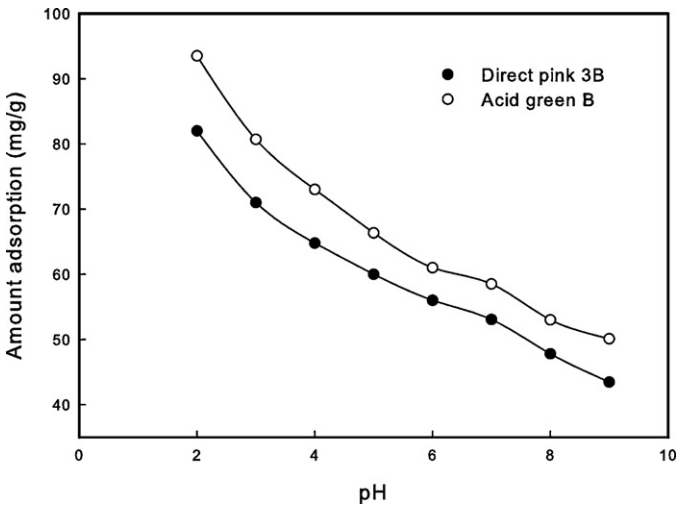

Fig. 6. Effect of the pH values on adsorption capacity of CA/OMMT nanocomposites for dyes. Conc.: 100 mg/L; temp.: 30 °C; *t*: 24 h.

B and direct pink 3B for C_0: 100 mg/L, in distilled water, *T*: 35 °C, *t*: 10 h. It is clear that wt% is an important factor affecting adsorption capacity of the nanocomposite. As it can be seen from Fig. 5, the adsorption capacity of the nanocomposite increased as 3% was introduced. The increase in dye adsorption with composite dosage can be attributed to increased adsorbent surface and the availability of more adsorption sites. However, if the adsorption capacity was expressed in mg adsorbed per gram of material, the capacity decreased with the increasing amount of composite. This may be attributed to overlapping or aggregation of adsorption sites resulting in a decrease in total adsorbent surface area available to the dye and an increase in diffusion path length (Crini et al., 2008).

3.4.2. Effect of pH

At lower pH more protons will be available to protonate hydroxyl groups of alginate, thereby increasing electrostatic attractions between negatively charged dye anions and positively charged adsorption sites and causing an increase in dye adsorption (Mahmoodi, Hayati, Arami, & Bahrami, 2011; Low & Lee, 1997). This explanation agrees with our data on pH effect. It can be seen that the pH of aqueous solution plays an important role in the adsorption of anionic dyes onto CA/OMMT. The CA contains hydroxyl group, –OH, which is easily protonated to form $–OH^{2+}$, in acidic solutions. The high adsorption capacity is due to the strong electrostatic interaction between the $–OH^{2+}$ of CA and dye anions (Yoshida, Okamoto, Kataoka, 1993).

The effect of pH on the adsorption of acid green B and direct pink 3B onto CA/OMMT is shown in Fig. 6. For two dyes, the adsorption capacity increases when the pH is decreased. For the CA/OMMT (3 wt%) nanocomposite, the decrease in the adsorption capacity reduced from pH 2.0 to pH 7.0 was 70.73 to 46 mg/g in direct dye and 90.6 to 40.44 mg/g in acid dye. Maximum adsorption of anionic dyes occurs at acidic pH (pH 2). At various pH values, the electrostatic attraction as well as the organic property and structure of dye molecules and CA/OMMT could play very important roles in dye adsorption on CA/OMMT. For lower pH the more positive the surface of the adsorbent (Calvete et al., 2009; Cardoso et al., 2011). At pH 2, a significantly high electrostatic attraction exists between the positively charged surface of the adsorbent, due to the ionization of functional groups of adsorbent and negatively charged anionic dye. As the pH of the system increases, the number of negatively charged sites is increased. A negatively charged site on the adsorbent does not favor the adsorption of anionic dyes due to the electrostatic repulsion (Kumar, 2000). Also, lower adsorption of two anionic dyes at alkaline pH is due to the presence of excess OH− ions destabilizing anionic dyes and competing with the dye anions for the adsorption sites. The effective pH was 2 and it was used in further studies. In order to continue the adsorption studies, the initial pH was fixed at 2.0. It should be stressed that the final pH of the adsorbate solution after the adsorption procedure did not changed remarkably. The final pH values of the adsorbate solutions were measured and its values attained up to 2.5.

3.4.3. Effect of temperature on adsorption

One of the important parameters which affect adsorption capacity is temperature. The effect of temperature on the adsorption of dyes (acid green B and direct pink 3B) on (CA/OMMT) nanocomposite is shown in (Table 1). The adsorption capacity of the nanocomposite increased with increasing *T* from 30 °C to 40 °C, and then it decreased with further increase in *T* from 40 °C to 50 °C. It is well known that increasing temperature may produce a swelling effect within the internal structure of adsorbent, leading to further penetrating for the large dye molecules (Bhattacharyya & Sarma, 2003). However, the mobility of the large dye ions increases with increasing temperature, which leads to a decrease in the adsorption capacity of nanocomposite with further increasing temperature. Results of sorption experiments showed that CA/OMMT

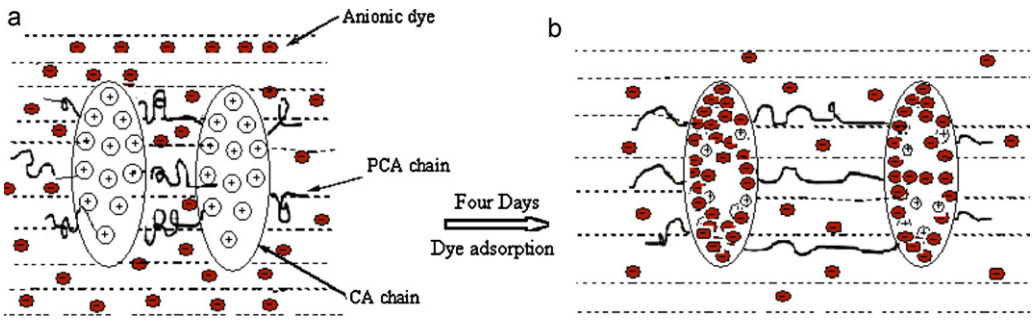

Fig. 7. Mechanism of dye adsorption onto CA/OMMT nanocomposites. (a) Before dye adsorption; (b) equilibrium condition.

nanocomposites exhibited high sorption capacities toward acid green B, which contains more than one sulfonate group.

A mechanism for the adsorption of anionic dyes on CA/OMMT nanocomposite is proposed (see Fig. 7). In the first step, the CA/OMMT is immersed in a solution with lower pH (pH 2.0), being the functional groups (OH, carboxylates) of the adsorbent protonated (see Fig. 7a). This step is fast. The second step is the separation of the agglomerates of dyes in the aqueous solution. Dyes are in an organized state in the aqueous solution, besides being hydrated (Cardoso et al., 2011). These self-associations of dyes in aqueous solutions should be dissociated before these dyes being adsorbed. Furthermore, the dyes should be dehydrated before being adsorbed. For acid green B, this step is relatively fast. The third stage is the electrostatic attraction of the negatively charged dyes by the positively surface charged CA/OMMT adsorbent at pH 2 (see Fig. 7b). This stage should be the rate controlling step.

3.4.4. Thermodynamic studies

Thermodynamic parameters related to the adsorption process, i.e., Gibb's free energy change (ΔG°, kJ mol^{-1}), enthalpy change (ΔH°, kJ mol^{-1}) and entropy change (ΔS°, J mol^{-1} K^{-1}) were obtained from the adsorption experiments at various temperatures (298, 308 and 318 K) and were estimated using below equations (Kamari & Ngah, 2009):

$$K_c = \frac{C_{Ad}}{C_e}$$

$$\Delta G = -RT \ln K_c$$

$$\ln K_c = \frac{\Delta S^\circ}{R} - \frac{\Delta H}{TR}$$

where K_c is the equilibrium constant, C_{Ad} (mg/L) is the concentration of dyes on solid at equilibrium, C_e is the equilibrium concentration of dyes in solution, R is the gas constant (8.314 J/kmol) and T is the temperature (K). The ΔH° and ΔS° values can be calculated from the slopes and intercepts of the Van't Hoff plot of $\ln K_c$ versus $1/T$. The use of the Van't Hoff plot is an indirect method to calculate thermodynamic adsorption parameters at solid/liquid interface (Zubieta et al., 2008). The thermodynamic results are depicted in Table 1. The R^2 values of the linear fit were at least 0.989 indicating that the values of enthalpy and entropy calculated for both adsorbents were confident. In addition, the magnitude of enthalpy was consistent with an electrostatic interaction of an adsorbent with an adsorbate (Kuo, Wu, & Wu, 2008) reinforcing the mechanism suggested in Fig. 7. The kind of interaction can be classified, to a certain extent, by the magnitude of enthalpy change. Physisorption, such as van der Waals interactions, are usually lower than 20 kJ mol^{-1}. Electrostatic interaction ranges from 20 to 80 kJ mol^{-1} and these kind of interactions are, frequently, classified as physisorption (Kuo et al., 2008). Chemisorption bond strengths can be 80–450 kJ mol^{-1} (Kuo et al., 2008). The negative value of enthalpy changes (ΔH°) confirms that the process of acid green B and direct pink 3B adsorption on CA/OMMT (3 wt%) are exothermic. Negative values of ΔG indicate that the investigated dyes adsorption by CA/OMMT adsorbents was a spontaneous and favorable process for all the studied temperatures. The positive values of ΔS° confirmed a high preference of anionic dyes on the surface of CA/OMMT nanocomposites, and also suggested the possibility of some structural changes or readjustments in the dye-carboxylate adsorption interaction. Besides, it is consistent with the dehydration of a dye molecule before its adsorption to carbon surface, and the release of these water molecules to the bulk solution, as also commented in the suggested mechanism discussed in Fig. 7. The increase in the adsorption capacities of CA/OMMT nanocomposites at higher temperatures may be attributed to the enhanced mobility and penetration of dye molecules within the adsorbent porous structures by overcoming the activation energy barrier and enhancing the rate of intra-particle diffusion (Asouhidou et al., 2009). The positive value of ΔS suggests the increased randomness at the solid/solution interface during the adsorption of dyes onto CA/OMMT.

3.5. Desorption studies

To evaluate the possibility of regeneration of CA/OMMT nanocomposites adsorbent, we have performed desorption experiments. Desorption study gives an idea about the nature of adsorption. Regeneration studies were carried out in order to know the reusability of the nanocomposites. The results of the studies indicated that the desorption of the adsorbed dyes in neutral distilled water resulted in about 5.52%, and 16.53% for acid green B and direct pink 3B, respectively. It is evident from the low desorption values, that the adsorption of dyes onto CA/OMMT nanocomposites (3 wt%) was chemisorption in nature. Chemisorption exhibits poor desorption probably due to the fact that in chemisorption the adsorbate species are held firmly to the adsorbent with comparatively stronger bonds. Therefore, the mechanisms of adsorption of dyes may be considered: electrostatic interaction between the cationic groups of OMMT and the anionic group of dye.

4. Conclusion

It can be concluded that the CA/OMMT nanocomposites can be successfully prepared by γ-ray irradiation polymerization. The improvement in thermal stability may attribute to the inherently good thermal properties of inorganic clays and the probable intercalation of polymer into interlamellar clay layers, prevents the heat to be transmitted quickly, and limited any further continuous decomposition of the nanocomposites. The particle size distribution ranges ≈ 87 nm the average equivalent particle size obtained from the TEM and referred to the OMMT nanocomposites are

randomly distributed and their particles are not equal uniformed throughout the OMMT particle matrix. Results of sorption experiments showed that CA/OMMT nanocomposites exhibited high sorption capacities toward acid green B, which contains more than one sulfonate group. Adsorption capacity of the investigated nanocomposites was found dependent on the pH and temperature of the aqueous dye solution. The thermodynamic data showed that dye adsorption onto CA/OMMT was spontaneous, exothermic, and a physisorption reaction. The results indicated that the organophilic montmorillonite may be an effective adsorbent for the removal of anionic dyes from wastewater.

References

Abou Taleb, M. F., Abd El-Mohdy, H. L. & Abd El-Rehim, H. A. (2009). Radiation preparation of PVA/CMC copolymers and their application in removal of dyes. *Journal of Hazardous Materials*, *168*, 68–75.

Al-Sigeny, S., Abou Taleb, M. F. & El-Kelesh, N. A. (2009). Hybrid nanocomposite prepared by graft copolymerization of 4-acryloyl morpholine onto chitosan in the presence of organophilic montmorillonite. *Journal of Macromolecular Science, Part A: Pure and Applied Chemistry*, *46*, 74–82.

Aravindhan, R., Fathima, N. N., Rao, J. R. & Nair, B. U. (2007). Equilibrium and thermodynamic studies on the removal of basic black dye using calcium alginate beads. *Colloids and Surfaces A*, *299*, 232–238.

Asouhidou, D. D., Triantafyllidis, K. S., Lazaridis, N. K., Matis, K. A., Kim, S. S. & Pinnavaia, T. J. (2009). Sorption of reactive dyes from aqueous solutions by ordered hexagonal and disordered mesoporous carbons. *Microporous and Mesoporous Materials*, *117*, 257–267.

Bhattacharyya, K. G. & Sarma, A. (2003). Adsorption characteristics of the dye, brilliant green, on neem leaf powder. *Dyes and Pigments*, *57*, 211–222.

Brookstein, D. S. (2009). Factors associated with textile pattern dermatitis caused by contact allergy to dyes, finishes, foams, and preservatives. *Dermatologic Clinics*, *27*, 309–322.

Calvete, T., Lima, E. C., Cardoso, N. F., Vaghetti, J. C. P., Dias, S. L. P. & Pavan, F. A. (2010a). Application of carbon adsorbents prepared from Brazilian-pine fruit shell for the removal of reactive orange 16 from aqueous solution: kinetic, equilibrium, and thermodynamic studies. *Journal of Environment Management*, *91*, 1695–1706.

Calvete, T., Lima, E. C., Cardoso, N. F., Dias, S. L. P. & Ribeiro, E. S. (2010b). Removal of brilliant green dye from aqueous solutions using homemade activated carbons. *Clean Soil Air Water*, *38*, 521–532.

Calvete, T., Lima, E. C., Cardoso, N. F., Dias, S. L. P. & Pavan, F. A. (2009). Application of carbon adsorbents prepared from the Brazilian-pine fruit shell for removal of Procion Red MX 3B from aqueous solution—Kinetic, equilibrium, and thermodynamic studies. *Chemical Engineering Journal*, *155*, 627–636.

Cardoso, N. F., Lima, E. C., Pinto, I. S., Amavisca, C. V., Royer, B., Pinto, R. B., et al. (2011). Application of cupuassu shell as biosorbent for the removal of textile dyes from aqueous solution. *Journal of Environment Management*, *92*, 1237–1247.

Carneiro, P. A., Umbuzeiro, G. A., Oliveira, D. P. & Zanoni, M. V. B. (2010). Assessment of water contamination caused by a mutagenic textile effluent/dyehouse effluent bearing disperse dyes. *Journal of Hazardous Materials*, *174*, 694–699.

Chen, H. & Wang, A. (2009). Adsorption characteristics of Cu_2 from aqueous solution onto poly(acrylamide)/attapulgite composite. *Journal of Hazardous Materials*, *165*(1-3), 223–231.

Crini, G., Robert, C., Gimbert, F., Martel, B., Adam, O. & De Giorgi, F. (2008). The removal of Basic Blue 3 from aqueous solutions by chitosan-based adsorbent: Batch studies. *Journal of Hazardous Materials*, *153*, 96–106.

Cuerda-Correa, E. M., Domínguez-Vargas, J. R., Olivares-Marín, F. J. & de Heredia, J. B. (2010). On the use of carbon blacks as potential low-cost adsorbents for the removal of non-steroidal anti-inflammatory drugs from river water. *Journal of Hazardous Materials*, *177*, 1046–1053.

Hummel, D. O. (1991). I. Band (Ed.), *Atlas of polymer and plastics analysis*. Munich, Vienna, New York, Barcelona: Hanser Publishers, pp. 243, 522.

Jankowski, T., Zielinska, M. & Wysakowska, A. (1997). Encapsulation of lactic acid bacteria with alginate/starch capsules. *Biotechnology Techniques*, *11*, 31–34.

Kamari, A. & Ngah, W. S. W. (2009). Isotherm, kinetic and thermodynamic studies of lead and copper uptake by H_2SO_4 modified chitosan. *Colloids and Surfaces B*, *73*, 257–266.

Kaşgöz, H. & Durmus, A. (2008). Dye removal by a novel hydrogel-clay nanocomposite with enhanced swelling properties. *Polymers for Advanced Technologies*, *19*(7), 838–845.

Kolhe, S. M. & Kumar, A. (2007). Radiation-induced grafting of vinyl benzyl trimethyl ammonium chloride onto nylon-6 fabric. *Radiation Physics and Chemistry*, *76*, 901–906.

Kumar, K. V., Ramamurthi, V. & Sivanesan, S. (2005). Modeling the mechanism involved during the sorption of methylene blue onto fly ash. *Journal of Colloid and Interface Science*, *284*, 14–21.

Kumar, M. N. V. R. (2000). A review of chitin and chitosan applications. *Reactive and Functional Polymers*, *46*, 1–27.

Kuo, C. Y., Wu, C. H. & Wu, J. Y. (2008). Adsorption of direct dyes from aqueous solutions by carbon nanotubes: Determination of equilibrium, kinetics and thermodynamics parameters. *Journal of Colloid and Interface Science*, *327*, 308–315.

Li, H., Yu, Y. & Yang, Y. (2005). Synthesis of exfoliated polystyrene/montmorillonite nanocomposite by emulsion polymerization using a zwitterion as the clay modifier. *European Polymer Journal*, *41*, 2016–2022.

Low, K. S. & Lee, C. K. (1997). Quaternized rice husk as sorbent for reactive dyes. *Bioresource Technology*, *121*, 121–125.

Mahmoodi, N. M., Hayati, B., Arami, M. & Bahrami, H. (2011). Preparation, characterization and dye adsorption properties of biocompatible composite (alginate/titania nanoparticle). *Desalination*, *275*, 93–101.

Malarvizhi, R. & Ho, Y. S. (2010). The influence of pH and the structure of the dye molecules on adsorption isotherm modeling using activated carbon. *Desalination*, *264*, 97–101.

Min, H., Wang, J., Hui, H. & Jie, W. (2006). Study on emulsion polymerization of PMMA/OMMT nano-composites by redox initiation. *Journal of Macromolecular Science, Part B: Physics*, *45*, 623–629.

Mulvancy, G. E. & Chang, D. M. (1977). Water-soluble copolymers containing *N*-vinylcarbazole. *Journal of Polymer Science, Polymer Chemistry Edition*, *15*(3), 585–591.

O¨ztop, H. N., Hepokur, C. & Saraydin, D. (2010). Poly (acrylamide/maleic acid)-sepiolite composite hydrogels for immobilization of invertase. *Polymer Bulletin*, *64*(1), 27–40.

Olivares-Marín, M., Del-Prete, V., Garcia-Moruno, E., Fernández-González, C., Macías-Garcí a, A. & Gmez-Serrano, V. (2009). The development of an activated carbon from cherry stones and its use in the removal of ochratoxin A from red wine. *Food Control*, *20*, 298–303.

Pulikesi, M., Ramamurthi, V. & Sivanesan, S. (2006). Equilibrium studies for the adsorption of acid dye onto modified hectorite. *Journal of Hazardous Materials*, *136*, 989–992.

Ramsay, J. A., Mok, W. H. W., Luu, Y. S. & Savage, M. (2005). Decoloration of textile dyes by alginate-immobilized trametes versicolor. *Chemosphere*, *61*, 956–964.

Royer, B., Cardoso, N. F., Lima, E. C., Macedo, T. R. & Airoldi, C. (2010). A useful organofunctionalized layered silicate for textile dye removal. *Journal of Hazardous Materials*, *181*, 366–374.

Royer, B., Cardoso, N. F., Lima, E. C., Vaghetti, J. C. P., Simon, N. M., Calvete, T., et al. (2009). Applications of Brazilian-pine fruit shell in natural and carbonized forms as adsorbents to removal of methylene blue from aqueous solutions—Kinetic and equilibrium study. *Journal of Hazardous Materials*, *164*, 1213–1222.

Sannino, A., Pappada', S., Madaghiele, M., Maffezzoli, A., Ambrosio, L. & Nicolais, L. (2005). Crosslinking of cellulose derivatives and hyaluronic acid with water-soluble carbodiimide. *Polymer*, *46*(25), 11206–11212.

Vijaya, Y., Popuri, S. R, Boddu, V. M. & Krishnaiah, A. (2008). Modified chitosan and calcium alginate biopolymer sorbents for removal of nickel (II) through adsorption. *Carbohydrate Polymers*, *72*, 261–271.

Weian, Z., Wei, L. & Yue'e, F. (2005). Synthesis and properties of a novel hydrogel nanocomposites. *Materials Letters*, *59*, 2876–2880.

Yi, J.-Z. & Zhang, L.-M. (2008). Removal of methylene blue dye from aqueous solution by adsorption onto sodium humate/polyacrlamide/clay hybrid hydrogels. *Bioresource Technology*, *99*(7), 2182–2186.

Yoshida, H., Okamoto, A. & Kataoka, T. (1993). Adsorption of acid dye on cross-linked chitosan fibers: Equilibria. *Chemical Engineering Science*, *48*, 2267–2272.

Zhou, M., Wei, Z., Qiao, H., Zhu, L., Yang, H. & Xia, T. (2009). Particle size and pore structure characterization of silver nanoparticles prepared by confined arc plasma. *Journal of Nanomaterials*, *5*, 1–5. Article ID 968058.

Zhu, L. & Ma, J. (2008). Simultaneous removal of acid dye and cationic surfactant from water by bentonite in one-step process. *Chemical Engineering Journal*, *139*, 503–509.

Zubieta, C. E., Messina, P. V., Luengo, C., Dennehy, M., Pieroni, O. & Schulz, P. C. (2008). Reactive dyes remotion by porous TiO_2–chitosan materials. *Journal of Hazardous Materials*, *152*, 765–777.